

Research Article

Novel Fractional Order Calculus Extended PN for Maneuvering Targets

Jikun Ye, Humin Lei, and Jiong Li

Air and Missile Defense College, Air Force Engineering University, Shaanxi, Xi'an 710051, China

Correspondence should be addressed to Jikun Ye; jikunbo@sina.com

Received 22 July 2016; Revised 30 November 2016; Accepted 18 December 2016; Published 12 January 2017

Academic Editor: Christopher J. Damaren

Copyright © 2017 Jikun Ye et al. This is an open access article distributed under the Creative Commons Attribution License, which permits unrestricted use, distribution, and reproduction in any medium, provided the original work is properly cited.

Based on the theory of fractional order calculus (FOC), a novel extended proportional guidance (EPN) law for intercepting the maneuvering target is proposed. In the first part, considering the memory function and filter characteristic of FOC, the novel extended PN guidance algorithm is developed based on the conventional PN after introducing the properties and operation rules of FOC. Further, with the help of FOC theory, the average load and ballistics characteristics of proposed guidance law are analyzed. Then, using the small offset kinematic model, the robustness of the new guidance law against autopilot parameters is studied theoretically by analyzing the sensitivity of the closed loop guidance system. At last, representative numerical results show that the designed guidance law obtains a better performance than the traditional PN for maneuvering target.

1. Introduction

The proportional navigation (PN) has been widely used because of its simplicity, ease of implementation, and effectiveness in practical systems [1–5]. Due to the fact that end of the line of sight (LOS) angular rate rapidly rotating easily leads to overload saturation when PN against maneuvering target, many scholars modified traditional PN guidance law to improve the performance of guidance law [6–9]. A Lyapunov method is used by Dhananjay to analyze the effect of LOS rate delay on the performance of PN guidance law in a head-on or tail-chase missile-target engagement scenario [10]; the author proposed the way for selecting the navigation gain to overcome the problem of LOS rate delay. Ghosh et al. derived a modified PN guidance law against higher speed nonmaneuvering targets to control terminal impact angle, which uses standard pure PN and retro-PN guidance laws in a 3D engagement scenario based on the initial engagement geometry and terminal engagement requirements. And the capture region of the new guidance law was researched [11]. Jeon and Lee modified PN for an ideal pursuer with a stationary target by obtaining an optimal feedback solution minimizing a performance index of the range-weighted control energy; the authors presented the exact analyses on optimality of PN based on a nonlinear formulation [12]. The

core idea of the above guidance law design is to add the compensation term against LOS rate delay, target maneuver, acceleration of gravity, and so on. The above studies centered on the integer order differential LOS rate, while the fractional calculus LOS rate has not been deeply researched and widely used.

With the development of fractional order calculus (FOC) theory, the FOC has been more and more widely used in engineering [13–15]. Considering the different application scenario, there are three common FOC definition: Riemann Liouville (RL) definition, Grunwald Letnikov (GL) definition, and Caputo definition [16, 17]. Zhang et al. discussed the order range of FOC and point out the differences of fractional order derivatives and integer order derivatives; the relations between RL definition, GL definition, and Caputo definition were studied too [18]. Unlike discontinuous change of integer order calculus, FOC expands calculus from the integer to fraction; the order of FOC can be changed continuously and reflects the nature of continuity better. The physical model established based on the FOC theory can describe physical phenomena with memory and time-dependent.

The major advantage of FOC is that it has fewer parameters and more simple forms; thus it is easy to be applied in reality. The specific memory functions and stability characteristics of fractional system have been more and more applied

in the area of guidance and control [19]. Considering that the atmospheric viscosity and interactions between air vehicles makes aircraft have aerodynamic properties of FOC, thus the FOC theory can describe the characteristics of the aircraft kinematic comprehensive and truly.

Sun and Zhu developed a new fractional order tension control law for the fast and stable deployment control problem of a space tether system and proved its stability [20]. Almeida and Torres presented a method to solve fractional optimal control problems, where the dynamic control system depended on integer order and Caputo fractional derivatives [21]. Vishal et al. used the theory of fractional order derivative to discuss the local stability of the Mathieu-van der Pol hyperchaotic system and studied the analysis of control time with respect to different fractional order derivatives [22].

Reference [23] studied the application of FOC controller for guided projectiles attitude control; the author concluded that fractional order control was better than classical PID control in robustness and control performance. Li et al. studied the stability of the fractional order unified chaotic system by the equivalent passivity method. With the FOC theory, the Lyapunov function was constructed by which it was proved that the controlled fractional order system was stable [24]. The FOC theory was introduced to the guidance area in reference [25]; the author employed the PD^λ guidance law to carry forward the advantages of traditional PN and avoid its drawbacks based on FOC theory and concluded that the PD^λ guidance had the higher guidance precision and shorter interception time. Zhu et al. proposed a modified FOC pure PN guidance law by means of Lyapunov-like method, which solved the control problem for the capture of a target with random maneuvers effectively [26]. However, the conclusion of [25, 26] was obtained in the two-dimensional plane under some certain conditions, so there were some strict restrictions on the designed guidance law, and this greatly limits its practical engineering applications.

This paper presents a novel 3D extended PN guidance algorithm for maneuvering target based on FOC theory, and it overcomes the disadvantage of PN. First, the basics knowledge and relative nature of FOC are outlined. Second, the proposed guidance law is given, which is composed of traditional LOS rate term and FOC LOS rate term. And the trajectory features, the load character, and the robustness of the new guidance law are analyzed theoretically. At last, simulations show that the proposed guidance law has superior performance, especially for a maneuvering target.

2. Preliminary Knowledge

The fractional calculus differential operator can be expressed as follows [13, 25]:

$${}_{\alpha}D_t^p = \begin{cases} \frac{d^p}{dt^p} & R(p) > 0 \\ 1 & R(p) = 0 \\ \int_0^t (dt)^{-p} & R(p) < 0, \end{cases} \quad (1)$$

where α, t denote the upper limit and lower limit respectively. p is the calculus operator, its value can be any plurality, and $R(p)$ presents the real part of p . If $p > 0$, then ${}_{\alpha}D_t^p$ denotes fractional derivative.

Definition 1. If the function $f(t)$ can be taken n order derivation, here $m - 1 \leq p < m$ and $n \in \mathbf{N}$, then we have the definition of Caputo derivative as follows:

$$D_t^p = \frac{1}{\Gamma(m-p)} \int_0^t \frac{f^m(\tau)}{(t-\tau)^{p-m+1}} d\tau, \quad (2)$$

where $\Gamma(x)$ denotes Gamma function, which is generalization of the factorial function $n!$, and we can take derivation of Gamma function with noninteger or even plurality. The expression of Gamma function can be denoted as

$$\Gamma(x) = \int_0^{\infty} t^{x-1} e^{-t} dt. \quad (3)$$

The Laplace transform of Caputo fractional derivative can be shown as

$$\begin{aligned} L[{}_0D_t^p f(t)] &= \int_0^{\infty} e^{-st} {}_0D_t^p f(t) dt \\ &= s^p F(s) - \sum_{k=0}^{n-1} s^{\alpha-k-1} f^k(0). \end{aligned} \quad (4)$$

In order to understand the links and differences between the integer order and fractional order calculus, we suppose that $f(t)$ is flat functions in the range $[a, t]$. Taking the derivation of $f(t)$ with n order, we have

$$f^n(t) = \lim_{h \rightarrow 0} \frac{1}{h^n} \sum_{j=0}^n (-1)^j \frac{n!}{j!(n-j)!} f(t-jh). \quad (5)$$

When the noninteger p replaces integer n and Γ function replaces binomial coefficients, we get the definition of Grunwald-Letnikov derivative as follows:

$$D_t^p f(t) = \lim_{h \rightarrow 0} \frac{1}{h^p} \sum_{j=0}^n (-1)^j \frac{\Gamma(p+1)}{j! \Gamma(p-j+1)} f(t-jh). \quad (6)$$

As can be seen from the above derivation, the most significant difference between integer order derivative and fractional derivative is that the former contains the recent information of several points, while the latter contains the past information of all the points. We can see that, from equation (6), the fractional derivative has the ability of memory function, and the closer the point, the stronger the impact factor [14].

In fact, the integer order calculus is a special case of fractional calculus, when the orders of fractional calculus $p \in \mathbf{N}$, the above two are equivalent. Another point to note is that FOC unifies the forms of the differential and integral expressions by fractional operator. When $p > 0$, it denotes fractional differential operator, while when $p < 0$, it represents fractional integral operator, so the study of integral and differential operation can be considered as an operator.

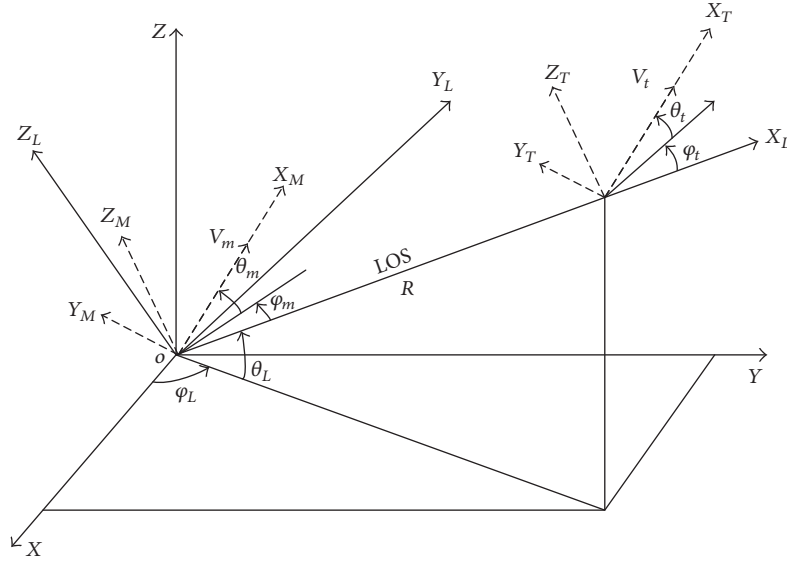


FIGURE 1: Pursuit geometry in 3-dimensional space.

Compared with the integer order linear system, the fractional linear system described by the FOC has the advantage of better memory function, better stability, and a greater choice of controller parameters.

3. Design of EPN Guidance Algorithm

We assume that the missile is an aerodynamic-controlled interceptor in a surface-to-air tactical missile defense scenario with a flat no rotating Earth. Consider a three-dimensional homing scenario shown in Figure 1, where M , T , and MT denote missile, target, and the missile-target LOS, respectively. The inertial frame is defined as $OXYZ$, and it is inertially fixed and centered at the launch site at the instant of launching. $OX_L Y_L Z_L$ denotes the LOS coordinate, r is the distance between missile and target, the relative velocity of missile and target is represented as V_r , and the elevation and azimuth of LOS are denoted by θ_L and φ_L , respectively. V_m is the velocity of missile, and θ_m and φ_m are the elevation and azimuth of V_m , respectively. And θ_t and φ_t are the elevation and azimuth of V_t , respectively.

According to the TPN law, the guidance command is defined as

$$\begin{aligned} U_a &= K_1 V_r \dot{\theta}_L, \\ U_b &= K_1 V_r \dot{\varphi}_L \cos \theta_L, \end{aligned} \quad (7)$$

where the guidance coefficient $K_1 > 2$ ensures convergent trajectory. $\dot{\theta}_L$ and $\dot{\varphi}_L$ denote the LOS rate, which can be obtained by detection system.

The conventional TPN consists of the relative velocity V_r , the LOS rate ($\dot{\theta}_L$ and $\dot{\varphi}_L$), and the proportional coefficient K_1 . V_r can be detected by the seeker and K_1 can be set in advance before launching the missile; the derivative of LOS angle (θ_L and φ_L) contains the information of instantaneous relative motion between missile and target. The instantaneous

LOS rate is used to calculate the load of TPN; however, the historical information of LOS rate is neglected, which may be useful to adjust the trajectory of missile. Considering that the derivative of FOC has unique historical memory effect, here we add the term of fractional order LOS rate to the guidance loop in order to carry forward the guidance effect of conventional TPN. In this way, the guidance command contains the more comprehensive information of relative motion to control the trajectory of missile.

Based on the theory of fractional order, here we construct a new form of EPN guidance law as follows:

$$U_a^p = K_1 V_r \dot{\theta}_L + K_1 V_r p D_t^p \theta_L, \quad (8)$$

$$U_b^p = K_1 V_r \dot{\varphi}_L \cos \theta_L + K_1 V_r D_t^p (\varphi_L) \cos \theta_L. \quad (9)$$

From (8) and (9), we find that the EPN guidance law is composed of two terms: one term is the traditional PN control, and the other term is fractional order differential of the LOS rotation rate. The fractional order term, used as compensation for the PN, contains the past information of LOS rotation rate. Note that when $p = 0$, the proposed EPN guidance law can be transformed to conventional PN guidance law.

4. Ballistic Characteristics Analysis of EPN Guidance Law

4.1. Characteristics Analysis of Average Overload. In order to simplify the expression of EPN, (7) can be rewritten as follows

$$\begin{aligned} U_a^p &= K_{a1} \dot{\theta}_L + K_{a2} D_t^p (\theta_L), \\ U_b^p &= K_{b1} \dot{\varphi}_L + K_{b2} D_t^p (\varphi_L), \end{aligned} \quad (10)$$

where $K_{a1} = K_1 V_r$, $K_{b1} = K_1 V_r \cos \theta_L$, $K_{a2} = K_1 V_r p$, and $K_{b2} = K_1 V_r D_t^p (\varphi_L) \cos \theta_L$.

According to the EPN expression, the average overload guidance law can be expressed as

$$\begin{aligned} \bar{U} &= \frac{1}{t_f} \int_0^{t_f} (U_a + U_b) dt = \frac{1}{t_f} \int_0^{t_f} (K_{a1} \dot{\theta}_L \\ &+ K_{a2} D_t^p(\theta_L) + K_{b1} \dot{\varphi}_L + K_{b2} D_t^p(\varphi_L)) dt = \frac{1}{t_f} \\ &\cdot \int_0^{t_f} K_{a1} \dot{\theta}_L dt + \frac{1}{t_f} \int_0^{t_f} K_{b1} \dot{\varphi}_L dt + \frac{1}{t_f} \\ &\cdot \int_0^{t_f} K_{b2} D_t^p(\varphi_L) dt + \frac{1}{t_f} \int_0^{t_f} K_{a2} D_t^p(\theta_L) dt \end{aligned} \quad (11)$$

Equation (11) can be simplified by the following term:

$$\begin{aligned} U_{a1} &= \frac{1}{t_f} \int_0^{t_f} K_{a1} \dot{\theta}_L dt, \\ U_{a2} &= \frac{1}{t_f} \int_0^{t_f} K_{a2} D_t^p(\theta_L) dt, \\ U_{b1} &= \frac{1}{t_f} \int_0^{t_f} K_{b1} \dot{\varphi}_L dt, \\ U_{b2} &= \frac{1}{t_f} \int_0^{t_f} K_{b2} D_t^p(\varphi_L) dt. \end{aligned} \quad (12)$$

The integration operation of U_{a1} , U_{a2} , U_{b1} , and U_{b2} with the interval $[0, t_f]$ (t_f represents the final time) yields

$$\begin{aligned} U_{a1} &= \frac{1}{t_f} \int_0^{t_f} K_{a1} \dot{\theta}_L dt = \frac{K_{a1} (\theta_{L_f} - \theta_{L_0})}{t_f}, \\ U_{b1} &= \frac{1}{t_f} \int_0^{t_f} K_{b1} \dot{\varphi}_L dt = \frac{K_{b1} (\varphi_{L_f} - \varphi_{L_0})}{t_f}, \\ U_{a2} &= \frac{1}{t_f} \int_0^{t_f} K_{a2} D_t^p(\theta_L) dt \\ &= \lim_{h \rightarrow 0} \frac{K_{a2}}{t_f} \int_0^{t_f} h^{-p} \sum_{j=0}^{\lfloor t/h \rfloor} \omega_j^p \dot{\theta}_L(t - jh) dt \\ &= \lim_{h \rightarrow 0} \frac{K_{a2}}{t_f} h^{-p} \sum_{j=0}^{\lfloor t/h \rfloor} \omega_j^p \int_0^{t_f} \dot{\theta}_L(t - jh) dt \\ &\approx \frac{K_{a2}}{t_f} h^{-p} \sum_{j=0}^{\lfloor t/h \rfloor} \omega_j^p (\theta_{L_f} - \theta_{L_0}). \end{aligned} \quad (13)$$

The following equation can be obtained according to operation of U_{a2} ,

$$U_{a2} = \bar{K}_{a2} \frac{(\theta_{L_f} - \theta_{L_0})}{t_f}, \quad (14)$$

where $\bar{K}_{a2} = (K_{a2}/t_f)h^{-p} \sum_{j=0}^{\lfloor t/h \rfloor} \omega_j^p$ and the subscripts 0 and f denote the initial state and final state, respectively.

The process of solving U_{b2} is similar to U_{a2} , so we have $U_{b2} = (\bar{K}_{b2} \varphi_{L_f} - \varphi_{L_0})/t_f$, where $\bar{K}_{b2} = (K_{b2}/t_f)h^{-p} \sum_{j=0}^{\lfloor t/h \rfloor} \omega_j^p$.

Let \bar{U}_a , \bar{U}_b denote the average pitch and lateral load, respectively; they can be expressed as

$$\begin{aligned} \bar{U}_a &= U_{a1} + U_{a2} = (K_{a1} + \bar{K}_{a2}) \frac{(\theta_{L_f} - \theta_{L_0})}{t_f} \\ \bar{U}_b &= U_{b1} + U_{b2} = (K_{b1} + \bar{K}_{b2}) \frac{(\varphi_{L_f} - \varphi_{L_0})}{t_f}. \end{aligned} \quad (15)$$

From the above operation, we get the average overload of EPN in the vertical plane as follows:

$$\begin{aligned} \bar{U} &= \bar{U}_a + \bar{U}_b \\ &= (K_{a1} + K_{a2}) \frac{(\theta_{L_f} - \theta_{L_0})}{t_f} \\ &+ (K_{b1} + K_{b2}) \frac{(\varphi_{L_f} - \varphi_{L_0})}{t_f}. \end{aligned} \quad (16)$$

Consider that the average overload of traditional TPN can be expressed as

$$\bar{U}_{\text{TPN}} = K_{\text{TPN1}} \frac{(\theta_{L_f} - \theta_{L_0})}{t_f} + K_{\text{TPN1}} \frac{(\varphi_{L_f} - \varphi_{L_0})}{t_f}, \quad (17)$$

where K_{TPN1} denotes the proportional coefficient of conventional PN. According to (16) and (17), we find that the average overload is closely related to change of LOS angle. The absolute value of average overload will increase as the LOS rotation rate becomes bigger. And calculations demonstrate that the average overload of EPN is closer to PN; it means that the ballistic controller's quantity of EPN is closer to PN.

4.2. Analysis of Required Overload. If we want to keep the trajectory of designed guidance law placidly and reduce the overload requirements of interceptor, the following conditions must be met:

$$\begin{aligned} |\theta_L - \theta_{L_0}| &\rightarrow \min, \\ |\theta_{L_f} - \theta_{L_0}| &\rightarrow \min, \\ |\theta_{L_f} - \theta_L| &\rightarrow \min, \\ |\varphi_L - \varphi_{L_0}| &\rightarrow \min, \\ |\varphi_{L_f} - \varphi_{L_0}| &\rightarrow \min, \\ |\varphi_{L_f} - \varphi_L| &\rightarrow \min. \end{aligned} \quad (18)$$

From (8), (9), and (18), the absolute load of EPN meets the following condition:

$$\begin{aligned} |U_a^p| &\leq K_{a1} |\dot{\theta}_L| + K_{a2} |D_t^p(\theta_L)|, \\ |U_b^p| &\leq K_{b1} |\dot{\varphi}_L| + K_{b2} |D_t^p(\varphi_L)|. \end{aligned} \quad (19)$$

From (19), we conclude that the maximum load of EPN can be denoted as follows:

$$\begin{aligned} \max \{U_a^p\} &\leq \max \{K_{a1}\dot{\theta}_L + K_{a2}D_t^p(\theta_L)\}, \\ \max \{U_b^p\} &\leq \max \{K_{b1}\dot{\varphi}_L + K_{b2}D_t^p(\varphi_L)\}. \end{aligned} \quad (20)$$

Note that, as the variation range of LOS angle is small, the trajectory of missile is closer to the straight line. When the LOS angle approaches zero, the acceleration of EPN $U_a^p \rightarrow 0$ and $U_b^p \rightarrow 0$. The extreme requirement loads in vertical and horizontal direction can be denoted as $N_{my} = \max\{|U_a|\}/g$ and $N_{mz} = \max\{|U_b|\}/g$. When $U_a^p \rightarrow 0$ and $U_b^p \rightarrow 0$, we have $N_{my} \rightarrow 0$ and $N_{mz} \rightarrow 0$. Thus, the proposed guidance EPN guidance law has the features of minimizing energy control and keeping trajectory straightly.

4.3. Characteristics Analysis of Ballistics. Considering the ups and downs of trajectory are closely related to the increment of LOS angle, if the LOS angles are controlled in a small range, the more flat trajectory can be obtained. Using this idea, compare the trajectory characteristic of EPN and PN by LOS angle changes during the process of flying. The lead angle of missile in pitch and lateral direction can be represented as follows:

$$\eta_m = \theta_L - \theta_m, \quad (21)$$

$$\varphi_m = \varphi_L - \varphi_m. \quad (22)$$

Considering the analysis process of trajectory in vertical plane is similar to the horizontal plane, here, we analyze the changes of lead angle in vertical plane only.

Taking the derivation of (21), we have

$$\dot{\eta}_m = \dot{\theta}_L - \dot{\theta}_m. \quad (23)$$

The ballistic inclination rate of missile can be denoted as

$$\begin{aligned} \dot{\theta}_m &= \frac{K_1 V_r \dot{\theta}_L + K_1 V_r p D_t^p(\theta_L)}{V_m} \\ &= K_{\theta 1} \dot{\theta}_L + K_{\theta 2} D_t^p(\theta_L). \end{aligned} \quad (24)$$

The integration of (23) for $t \in [0, t_f]$ yields

$$\begin{aligned} \eta_{mf} &= \eta_{m0} + (1 - K_{\theta 1})(\theta_{Lf} - \theta_{L0}) \\ &\quad - K_{\theta 2} \int_0^{t_f} D_t^p(\dot{\theta}_L) dt \\ &= \eta_{m0} + (1 - K_{\theta 1})(\theta_{Lf} - \theta_{L0}) \\ &\quad - K_{\theta 2} h^{-p} \sum_{j=0}^{\lfloor t/h \rfloor} \omega_j^p (\theta_{Lf} - \theta_{L0}). \end{aligned} \quad (25)$$

Let $\bar{K}_{\theta 2} = K_{\theta 2} h^{-p} \sum_{j=0}^{\lfloor t/h \rfloor} \omega_j^p$. Substituting $\bar{K}_{\theta 2}$ to (25) results in

$$\begin{aligned} \eta_{mf} &= \eta_{m0} + (1 - K_{\theta 1})(\theta_{Lf} - \theta_{L0}) \\ &\quad - \bar{K}_{\theta 2} (\theta_{Lf} - \theta_{L0}). \end{aligned} \quad (26)$$

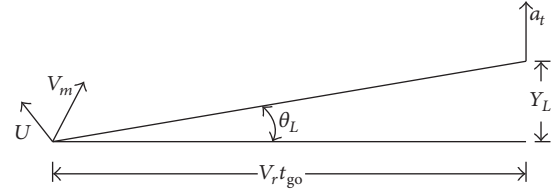


FIGURE 2: Illustration of small offset motion.

When $\eta_{m0} = 0$, the following equations can be obtained based on (26):

$$\theta_{Lf} - \theta_{L0} = \frac{\eta_{mf}}{K_{\theta 1} + \bar{K}_{\theta 2} - 1}. \quad (27)$$

For the traditional PN guidance law, the lead angle changes in vertical plane can be denoted as follows:

$$\theta_{Lf} - \theta_{L0} = \frac{\eta_{mf}}{K_{\theta 1} - 1}. \quad (28)$$

According to (27) and (28), we find that the introduced fractional order term of EPN further increases the trajectory smoothness by decreasing the variation range of ballistic elevation. So the trajectory of EPN can be controlled easily and the requirements of actuator design reduced greatly. Considering the analysis in horizontal is similar to the vertical, therefore we no longer study it.

4.4. Robustness Analysis of EPN against Autopilot. Figure 2 shows the kinematic relation of small offset.

By using the approximation $\sin \theta_L \approx \theta_L$ (this approximation is rational because Y_L is small offset), we have

$$\theta_L = \frac{Y_L}{V_r t_{go}}, \quad (29)$$

where t_{go} denotes time-to-go; the solution of the differential equation (29) can be obtained as

$$\dot{\theta}_L = Y_L + \frac{\dot{Y}_L t_{go}}{V_r t_{go}^2}. \quad (30)$$

The transform function of autopilot can be expressed as follows:

$$G(s) = \frac{b_m s^m + b_{m-1} s^{m-1} + \dots + b_1 s + 1}{a_n s^n + a_{n-1} s^{n-1} + \dots + a_1 s + 1} \quad (n > m) \quad (31)$$

Taking the terminal homing guidance as an example, the guidance loop of small offset model can be denoted as Figure 3. Note that, comparing with traditional PN guidance loop, the EPN increases the fractional order term which is parallel with the PN term in the homing guidance loop.

Let $U_y(s)/Y(s) = G_y(s)$; according to the properties of fractional order, we have

$$\begin{aligned} L[D_t^p f(t)] &= s^p L[f(t)] - \sum_{k=1}^{n-1} s^k [D_t^{p-k-1} f(t)]_{t=0} \\ &\approx s^\lambda \frac{1 + st_{go}}{V_r t_{go}^2} - s^0 h^{-p} \sum_{j=0}^{[t/h]} \omega_j^{-1} f(0) \\ &\quad - s^1 h^{-p} \sum_{j=0}^{[t/h]} \omega_j^{p-2} f(0). \end{aligned} \quad (32)$$

The transfer function $G_y(s)$ can be obtained as

$$\begin{aligned} G_y(s) &= K_{a1} \frac{1 + st_{go}}{V_r t_{go}^2} + s^p \frac{1 + st_{go}}{V_r t_{go}^2} \\ &\quad + h^{-p} \sum_{j=0}^{[t/h]} \omega_j^{p-1} \frac{2 + st_{go}}{V_r t_{go}^3} \\ &\quad + h^{-p} \sum_{j=0}^{[t/h]} \omega_j^{p-2} \frac{s + s^2 t_{go}}{V_r t_{go}^3}. \end{aligned} \quad (33)$$

The guidance loop transfer coefficient of EPN can be expressed as

$$\begin{aligned} K_{FOCPN}^y &= \lim_{s \rightarrow 0} s^2 \frac{1}{s^2} G_y(s) G(s) \\ &= \frac{1}{V_r t_{go}^3} (K_{a1} t_{go} + 2\bar{K}_{a2}), \end{aligned} \quad (34)$$

where $\bar{K}_{a2} = K_{a2} h^{-p} \sum_{j=0}^{[t/h]} \omega_j^p$.

The guidance loop transfer coefficient of PN and PD (proportional differential) guidance law can be denoted, respectively, as follows:

$$\begin{aligned} K_{PN}^y &= \frac{K_1 t_{go}}{V_r t_{go}^3}, \\ K_{PD}^y &= \frac{(K_{a1} t_{go} + 2K_{a2})}{V_r t_{go}^3}. \end{aligned} \quad (35)$$

Comparing the transfer coefficients of EPN with PN and PD, we have

$$K_{FOCPN}^y > K_{PD}^y > K_{PN}^y \quad (36)$$

The conclusion of transfer coefficients in horizontal plane is similar to the vertical plane; the relationship can be expressed as

$$K_{FOCPN}^x > K_{PD}^x > K_{PN}^x. \quad (37)$$

According to (36) and (37), we can see the guidance ability against maneuvering target strengthened as a result of increasing the gain coefficients of transfer function by the introduction of fractional order term. So the guidance systematic errors will be reduced and the guidance accuracy will be improved in some sense.

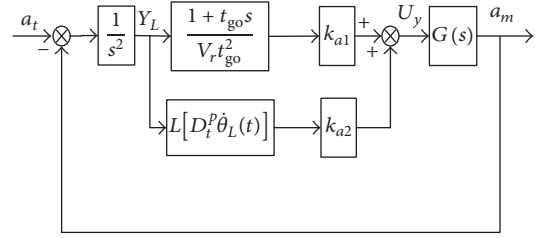


FIGURE 3: Illustration of the closed loop EPN guidance system.

Definition 2. The sensitivity of systems T against coefficient K is defined as follows:

$$S_K^T = \frac{d(\ln(T))}{d(\ln(K))}. \quad (38)$$

The sensitivity of stability guidance system against the coefficients K_{a1} and K_{a2} can be calculated as follows:

$$\begin{aligned} S_{K_{a1}}^e &= -\frac{K_{a1} t_{go}}{K_{a1} t_{go} + 2K_{a1}}, \\ S_{K_{a2}}^e &= -\frac{K_{a2}}{K_{a1} t_{go} + 2K_{a1}}. \end{aligned} \quad (39)$$

When using traditional PN guidance, the sensitivity $S_{K_1}^e = -1$. In contrast with formula (39), we have $|S_{K_1}^e| > |S_{K_{a1}}^e|$, $|S_{K_1}^e| > |S_{K_{a2}}^e|$; this means that the sensitivity of EPN guidance against each coefficient (K_{a1}, K_{a2}) is smaller than PN guidance. Thus, the proposed EPN guidance law has a stronger response against parameter changes.

According to the homing guidance system loop in Figure 3, the differential functions of system transmission error can be obtained

$$\frac{dG_e(s)}{dG(s)} = -\frac{s^2 G_1(s)}{[s^2 + G_1(s)G(s)]^2},$$

$$\frac{dG(s)}{db_i} = \frac{s^i}{P(s)}, \quad i = 1, 2, \dots, m, \quad (40)$$

$$\frac{dG(s)}{da_j} = -\frac{G(s)s^j}{P(s)}, \quad j = 1, 2, \dots, n,$$

where $P(s)$ is the intermediate computing term; therefore, according to (40), we obtain

$$S_{b_i}^e = E(s) \frac{b_i s^i}{P(s)}, \quad i = 1, 2, \dots, m, \quad (41)$$

$$S_{a_j}^e = -E(s) G(s) \frac{a_j s^j}{P(s)}, \quad j = 1, 2, \dots, n,$$

where $E(s) = -G(s)/(s^2 + G_1(s)G(s))$; as $s = 0$, we have

$$\left. \frac{S_{b_i}^e}{s^i} \right|_{s=0} = -\frac{b_i}{K_{a1} t_{go} + 2K_1}, \quad i = 1, 2, \dots, m,$$

$$\left. \frac{S_{a_j}^e}{s^j} \right|_{s=0} = -\frac{a_j}{K_{a1} t_{go} + 2K_1}, \quad j = 1, 2, \dots, n,$$

TABLE 1: Engagement specifications.

Parameters of missile and target	
$(X_{m_0}, Y_{m_0}, Z_{m_0})$	(0, 0, 0) km
$(X_{t_0}, Y_{t_0}, Z_{t_0})$	(10, 10, 10) km
θ_t	0
φ_t	180
θ_m	36
φ_m	45
V_m	800
V_t	400

$$\begin{aligned} \frac{S_{b_i}^e}{s^i} \Big|_{s=0}^{\text{PN}} &= -\frac{b_i}{K_{a1} t_{\text{go}}}, \quad i = 1, 2, \dots, m, \\ \frac{S_{a_j}^e}{s^j} \Big|_{s=0}^{\text{PN}} &= -\frac{a_j}{K_{a1} t_{\text{go}}}, \quad j = 1, 2, \dots, n. \end{aligned} \quad (42)$$

It can be seen from (42) that the absolute sensitivity of EPN against autopilot parameter decreases because of the increase in denominator by introducing the fractional term. Therefore, the robustness of EPN against autopilot parameter changes is more robust than PN guidance.

5. Simulation Results and Analysis

In this section, some results of simulation are presented for 3D engagement to verify the performance of the designed EPN, simulation initial step is 0.01 s, and the proportional coefficient is taken as 3.5. Some other initial parameters of missile and target are shown in Table 1. The airframe dynamics including autopilot has been modeled as a second-order system with time lag as described by [27]. The total autopilot lag is modeled as

$$T = \frac{\omega_n^2}{(\tau s + 1)(s^2 + 2\zeta\omega_n s + \omega_n^2)}, \quad (43)$$

where the autopilot parameters are $\tau = 0.5$ s, $\zeta = 0.6$, and $\omega_n = 18$ rad/s. Due to the order of FOC in the range [0, 1], according to traverse optimization methods, the optimum value of differential order p is taken as 0.6. Consider that the LOS rate is contaminated with uncertainty during the terminal guidance phase, and we assume that the measurement error of the onboard seeker is 0.01 deg/s.

To investigate the performance of the proposed guidance law efficiently, three cases of simulations are carried out: (1) the target with no maneuver; (2) the target maneuver in the inclined plane with the acceleration 40 m/s²; (3) the target maneuver in a snake-like mode with the acceleration 20 m/s² in both the vertical and horizontal planes.

The comparison of the interception performances between the EPN guidance law and PN guidance law is presented in Table 2, where MD is the mean miss distance, defined as the closest distance between the missile and

TABLE 2: Comparison of the interception performance.

	Guidance law	MD/m	ET/s
Case 1	PN	1.2129	35.55
	EPN	0.6272	35.05
Case 2	PN	3.9193	33.34
	EPN	1.978	32.89
Case 3	PN	2.3398	40.55
	EPN	1.178	40.32

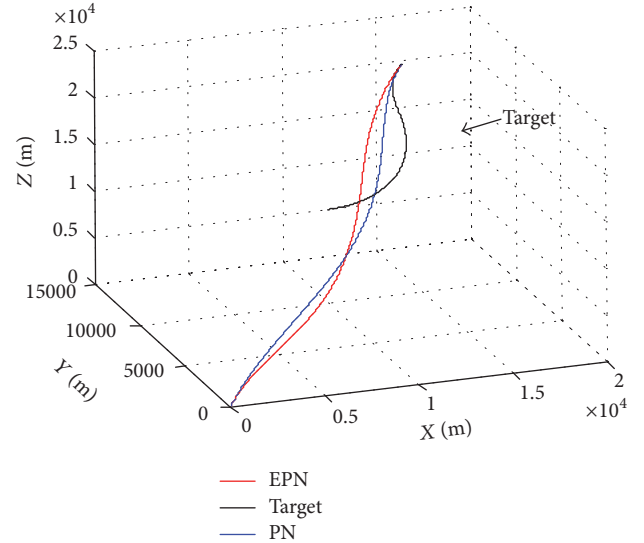


FIGURE 4: Trajectories of missile and target.

the target before divergence, and where ET denotes the engagement time. All performance results are based on 200 run Monte-Carlo simulations.

Small miss distance is the most important in the homing guidance. According to the simulation results shown in Table 2, both of the conventional PN and the proposed EPN guidance law are able to intercept targets effectively. However, the guidance precision of EPN is nearly 50% better than the PN guidance, which indicates that the EPN has greatly improved the guidance accuracy. It is also interesting to note that the engagement time of EPN is always shorter than PN, which means that the EPN will shot down the target earlier than PN.

In order to describe the guidance character of acceleration and ballistic trajectory, we give the simulation figures of case 3 only, which are shown as Figures 4–8.

As can be seen from Figure 4, the trajectory of the EPN is smoother than the PN. The curvature of the missile's trajectory guided by EPN is smaller than PN, especially in the end of engagement, which is in favor of ballistic control. As illustrated in Figures 5 and 6, the main difference between EPN and PN is the adjustment rate of elevation and azimuth. In the initial phase of engagement, the proposed EPN adjusts its attitude quicker than PN and this makes the trajectory of EPN smoother in the later stage of interception. Figures 7 and 8 denote that the acceleration of the PN guidance law tends

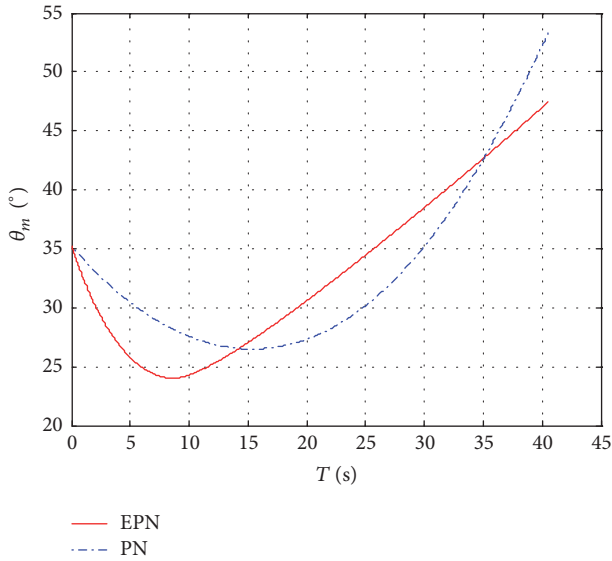


FIGURE 5: Time history of trajectory elevation.

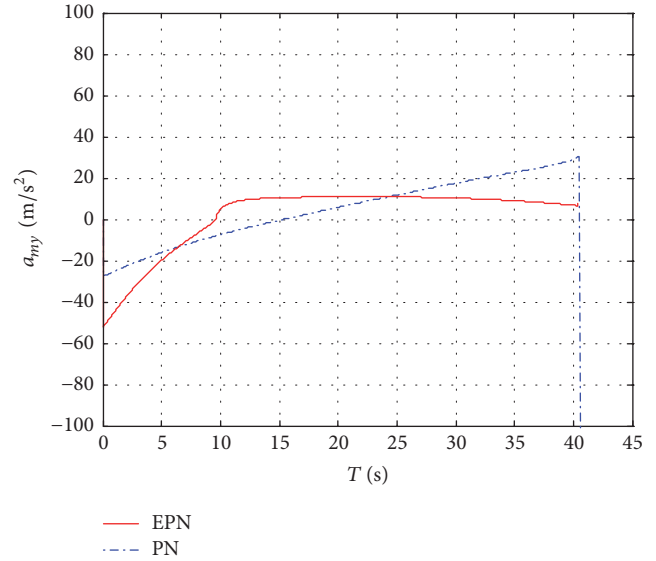


FIGURE 7: Time history of normal acceleration.

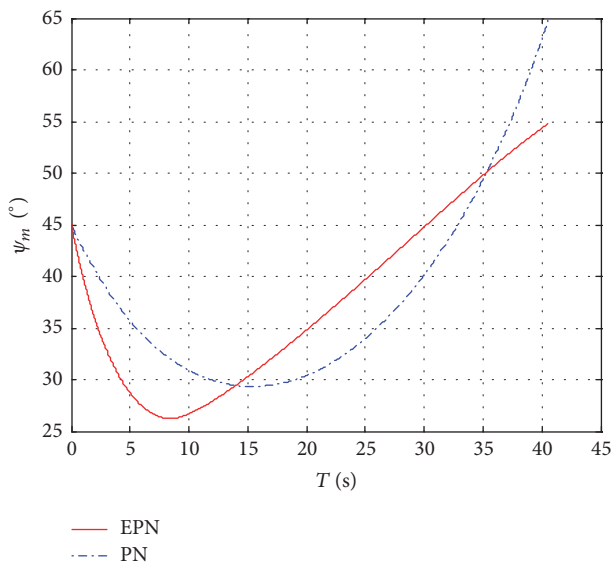


FIGURE 6: Time history of trajectory azimuth.

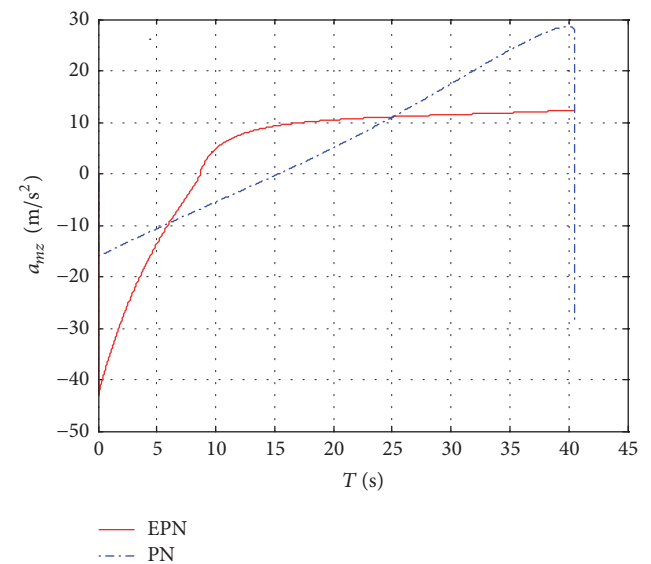


FIGURE 8: Time history of lateral acceleration.

to achieve its saturation which compensates for the target's maneuver at the end, whereas the loads of EPN undergoes a relatively stable tendency during the engagement, which positively adjusts the missile attitude at the expense of loads in the initial phase of interception without dramatic increase at the end. So the load of EPN undergoes a relatively stable tendency during the flight envelope, while the load of PN diverges at the point of impact caused by the divergence of LOS rate.

With respect to the PN guidance law, the proposed EPN guidance law maintains the tracking performance and exhibit more favorable guidance performance in intercepting maneuvering target. In fact, EPN solves the problem of LOS rate estimation by the fractional order differential treatment of LOS rate. In other words, the fractional order differential

controller plays the role of filter, which improves the control precision and stability of the guidance system. In a word, the EPN extends the guidance performance of missile by carrying forward the advantages of PN guidance law and avoids its shortcomings in some sense.

6. Conclusions

To improve the performance of conventional PN guidance, this paper proposed a novel EPN guidance law based on the fractional order calculus theory. The guidance characteristics of EPN, such as average load, trajectory stability, and robustness, are analyzed theoretical. The inducement of fractional order term extended the performance of PN greatly especially in the guidance precision and interception

time and overcome the load saturation caused by LOS rate divergence in the end of engagement. And the EPN guidance law has more flexible structure and better robustness. Extensive simulations of various engagements demonstrate that the proposed guidance law provides satisfactory performance against maneuvering targets.

The proposed guidance law is designed with the consideration of maneuvering target in the atmosphere; however, the guidance law needs further analysis, especially to achieve direct collision interception in the near space against hypersonic target.

Competing Interests

The authors declare that there is no conflict of interests regarding the publication of this paper.

Acknowledgments

The first author would like to thank the Air and Missile Defense College of Air Force Engineering University of China for giving permission for conducting guidance research at the laboratory. This work was supported by National Natural Science Foundation of China (nos. 61573374, 61503408, and 61603410) and Aviation Science Innovation Foundation of China (no. 20150196006).

References

- [1] L. Chen and B. Zhang, "Novel TPN control algorithm for exoatmospheric intercept," *Journal of Systems Engineering and Electronics*, vol. 20, no. 6, pp. 1290–1295, 2009.
- [2] Q. Z. Zhang, Z. B. Wang, and F. Tao, "Optimal guidance law design for impact with terminal angle of attack constraint," *Optik*, vol. 125, no. 1, pp. 243–251, 2014.
- [3] K. Li, L. Chen, and X. Bai, "Differential geometric modeling of guidance problem for interceptors," *Science China Technological Sciences*, vol. 54, no. 9, pp. 2283–2295, 2011.
- [4] J. Ye, H. Lei, D. Xue, J. Li, and L. Shao, "Nonlinear differential geometric guidance for maneuvering target," *Journal of Systems Engineering and Electronics*, vol. 23, no. 5, pp. 752–760, 2012.
- [5] F. Tyan, "Unified approach to missile guidance laws: a 3D extension," *IEEE Transactions on Aerospace and Electronic Systems*, vol. 41, no. 4, pp. 1178–1199, 2005.
- [6] K. Li, T. Zhang, and L. Chen, "Ideal proportional navigation for exoatmospheric interception," *Chinese Journal of Aeronautics*, vol. 26, no. 4, pp. 976–985, 2013.
- [7] S.-C. Han, H. Bang, and C.-S. Yoo, "Proportional navigation-based collision avoidance for UAVs," *International Journal of Control, Automation and Systems*, vol. 7, no. 4, pp. 553–565, 2009.
- [8] C.-Y. Li and W.-X. Jing, "Geometric approach to capture analysis of PN guidance law," *Aerospace Science and Technology*, vol. 12, no. 2, pp. 177–183, 2008.
- [9] Y. Xia and M. Fu, "Missile guidance laws based on SMC and FTC techniques," in *Compound Control Methodology for Flight Vehicles*, vol. 438 of *Lecture Notes in Control and Information Sciences*, pp. 211–224, Springer, Berlin, Heidelberg, 2013.
- [10] N. Hananjay, K.-Y. Lum, and J.-X. Xu, "Proportional navigation with delayed line-of-sight rate," *IEEE Transactions on Control Systems Technology*, vol. 21, no. 1, pp. 247–253, 2013.
- [11] S. Ghosh, D. Ghose, and S. Raha, "Three dimensional PN based impact angle control for higher speed nonmaneuvering targets," in *Proceedings of the American Control Conference (ACC '13)*, pp. 31–36, Washington, DC, USA, June 2013.
- [12] I.-S. Jeon and J.-I. Lee, "Optimality of proportional navigation based on nonlinear formulation," *IEEE Transactions on Aerospace and Electronic Systems*, vol. 46, no. 4, pp. 2051–2055, 2010.
- [13] R. Caponetto, G. Dongola, and L. Fortuna, *Fractional Order Systems: Modeling and Control Applications*, World Scientific, Singapore, 2010.
- [14] Q. Zeng, G. Cao, and X. Zhu, "Research on controllability for a class of fractional-order linear control systems," *Journal of Systems Engineering and Electronics*, vol. 16, no. 2, pp. 376–381, 2005.
- [15] I. P. Cristina, I. Clara, D. K. Robain, and E. H. Dulf, "Robustness evaluation of fractional order control for varying time delay processes," *Signal, Image and Video Processing*, vol. 6, no. 3, pp. 453–461, 2012.
- [16] K. S. Miller and B. Ross, *An Introduction to the Fractional Calculus and Fractional Differential Equations*, A Wiley-Interscience Publication, John Wiley & Sons, New York, NY, USA, 1993.
- [17] S. G. Smako, A. A. Kilbas, and O. I. Marichev, *Fractional Integrals and Derivatives, Theory and Applications*, Gordon and Breach Science Publishers, New York, NY, USA, 1987.
- [18] X.-X. Zhang, T.-S. Qiu, and H. Sheng, "A physical interpretation of fractional calculus and fractional calculus with constant extent of integral," *Acta Electronica Sinica*, vol. 41, no. 3, pp. 508–512, 2013.
- [19] A. A. Kilbas, H. M. Srivastava, and J. J. Trujillo, *Theory and applications of fractional differential equations*, vol. 204 of *North-Holland Mathematics Studies*, Elsevier Science B.V., Amsterdam, Netherlands, 2006.
- [20] G. Sun and Z. H. Zhu, "Fractional-order tension control law for deployment of space tether system," *Journal of Guidance, Control, and Dynamics*, vol. 37, no. 6, pp. 2057–2061, 2014.
- [21] R. Almeida and D. F. M. Torres, "A discrete method to solve fractional optimal control problems," *Nonlinear Dynamics*, vol. 80, no. 4, pp. 1811–1816, 2015.
- [22] K. Vishal, S. K. Agrawal, and S. Das, "Hyperchaos control and adaptive synchronization with uncertain parameter for fractional-order Mathieu-van der Pol systems," *Pramana*, vol. 86, no. 1, pp. 59–75, 2016.
- [23] J.-G. Shi, Z.-Y. Wang, S.-J. Chang, and B.-S. Zhang, "Fractional-order control systems for guided projectiles," *Journal of Nanjing University of Science and Technology (Natural Science)*, vol. 35, no. 1, pp. 52–56, 2011.
- [24] T.-Z. Li, Y. Wang, and M.-K. Luo, "Control of fractional chaotic and hyperchaotic systems based on a fractional order controller," *Chinese Physics B*, vol. 23, no. 8, Article ID 080501, 2014.
- [25] F. Wang and H. M. Lei, "PD^λ guidance law based on fractional calculus," *Control Theory & Applications*, vol. 27, no. 1, pp. 126–130, 2010.
- [26] Z.-T. Zhu, Z. Liao, C. Peng, and Y. Wang, "A fractional-order modified proportional navigation law," *Control Theory & Applications*, vol. 29, no. 7, pp. 945–949, 2012.
- [27] S. Rituraj, N. Prabhakar, A. K. Sarkar et al., "Three dimensional nonlinear inverse dynamics guidance law for parallel navigation," in *Proceedings of the AIAA Guidance, Navigation, and Control Conference and Exhibit*, pp. 1–8, Providence, RI, USA, 2004.



Hindawi

Submit your manuscripts at
<https://www.hindawi.com>

